

An improved single-column model representation of ocean mixing associated with summertime leads: Results from a SHEBA case study

Marika M. Holland

National Center for Atmospheric Research, Boulder, Colorado, USA

Received 19 July 2002; revised 7 November 2002; accepted 24 January 2003; published 2 April 2003.

[1] Ice/ocean mixed layer model simulations are run for a SHEBA field project case study from 5 July–8 August 1998. Observations indicate that during this time, calm winds occurred and coincided with a rapid warming and freshening of the surface of a lead near the SHEBA camp. A subsequent storm mixed down this warm, fresh water. Single-column model simulations of this event are performed to isolate properties of the ocean system which must be accounted for to improve the representation of mixing in summertime leads. A traditional method of simulating the ice/ocean system in which a single ocean mixed layer calculation is forced with fluxes aggregated over the ice and open water portions of the domain is compared with simulations in which separate mixed layer calculations are done for the lead and under-ice ocean systems. It is found that not only are multiple ocean mixed layer calculations needed to improve the simulations but the surface of the lead must be realistically embedded within the ice cover. When stable conditions occur, the lead surface remains isolated from the under-ice system. Using this method considerably improves simulated lead vertical temperature and salinity profiles, allowing the lead surface to freshen to 20 ppt and reach temperatures greater than 1.4°C above freezing. This modifies the ice mass budgets, increasing lateral melt rates, open water formation, and the amount of absorbed solar radiation. This has implications for the accurate simulation of climate change and variability due to its effects on the albedo feedback mechanism. *INDEX TERMS*: 4540 Oceanography: Physical: Ice mechanics and air/sea/ice exchange processes; 4207 Oceanography: General: Arctic and Antarctic oceanography; 4255 Oceanography: General: Numerical modeling; *KEYWORDS*: ocean leads, ice/ocean exchange, SHEBA, sea ice, summer ice cover

Citation: Holland, M. M., An improved single-column model representation of ocean mixing associated with summertime leads: Results from a SHEBA case study, *J. Geophys. Res.*, 108(C4), 3107, doi:10.1029/2002JC001557, 2003.

1. Introduction

[2] Open-water leads are relatively narrow cracks in the ice cover through which the atmosphere is in direct contact with the polar oceans. Although these leads and the thin ice produced in the leads occupy a relatively small area, they dominate the heat exchange in winter [Maykut, 1982]. In the summer the presence of leads reduces the surface albedo and increases the solar radiation that is absorbed in the ocean mixed layer. It appears that this process is responsible for a majority of the warming of the surface ocean and the consequent ice/ocean heat exchange in the Arctic [Maykut and Perovich, 1987; Maykut and McPhee, 1995]. As such, the magnitude of this flux has implications for the ice mass budgets. Additionally, the fractional coverage of leads plays a role in the positive ice-albedo feedback which modifies climate change and variability [e.g., IPCC, 2001].

[3] Because of these effects, it is important for climate models to accurately simulate leads and the processes associated with them. The sea ice components used in climate simulations have improved in recent years. For example,

version 2 of the Community Climate System Model (CCSM2) includes a sea ice model with an elliptical yield curve rheology and a subgridscale ice thickness distribution. The model explicitly calculates lead opening due to dynamic and thermodynamic processes. However, in this model (and atmosphere and ocean general circulation models in general), the ocean and atmospheric boundary layers do not differentiate between lead and ice covered regions. Instead fluxes are aggregated over lead and ice covered fractions of the grid cell, and the model implicitly assumes that the ice covered and open ocean regions of a grid cell are well mixed.

[4] Observations suggest that there are subgridscale processes associated with leads that affect ocean and atmospheric stability and vertical mixing. For example, summertime measurements from the Surface Heat Budget of the Arctic (SHEBA) field program indicate that during a period of calm winds, leads in the vicinity of the SHEBA camp rapidly warmed and freshened at the surface [Paulson and Pegau, 2001; Richter-Menge et al., 2001; W. S. Pegau and C. A. Paulson, The summertime thermohaline evolution of an Arctic lead, to be submitted to *Journal of Geophysical Research*, 2003, hereinafter referred to as Pegau and Paulson, submitted manuscript, 2003]. The warm, fresh water was subsequently mixed downward under the ice when high

winds occurred. These conditions influenced the basal and lateral melting of the ice cover [Perovich *et al.*, 2003], the open water formation, and hence the surface albedo. Ocean general circulation models (OGCMs) which do not differentiate between the lead and under-ice conditions cannot capture these effects. Additionally, previous studies which concluded that lateral melting was relatively unimportant for the central Arctic sea ice mass budget [Steele, 1992] assumed that the water in leads and under the sea ice were well mixed and thus did not capture the types of conditions observed during SHEBA.

[5] The subgridscale effects of leads are similarly important for the atmosphere. During winter, the turbulent heat loss from leads are typically two orders of magnitude larger than those over the surrounding ice cover [Badgley, 1966]. The large heat and water fluxes emanating from the leads can result in cloud formation which may be quite extensive and have important radiative effects [e.g., Serreze *et al.*, 1992; Pinto *et al.*, 1995]. Additionally, elevated turbulent fluxes can persist for several days after the lead surface has refrozen [Pinto *et al.*, 2003] owing to the presence of thin newly formed sea ice.

[6] The purpose of this study is to determine properties of the ice-ocean system which must be accounted for to improve the simulation of summertime leads for climate modeling applications. Previous studies [Morison *et al.*, 1992; Kantha, 1995; McPhee and Stanton, 1996; Smith and Morison, 1998; Skillingstad and Denbo, 2001] have used observations, two-dimensional turbulence closure modeling, and large eddy simulations to investigate the oceanography of winter leads. These studies have been instrumental in improving our understanding of ocean turbulence and mixing in the polar seas. However, they do not consider summertime conditions, and the complexity of the modeling studies makes it difficult to extend the results to the relatively simple parameterizations needed for climate modeling. A different approach is used here in that climate model components are used in a single-column modeling framework with different configurations to determine the important features that must be included to obtain the type of conditions that were observed during SHEBA. As climate model components are used for this study, the results should provide guidance on how to improve lead processes within these models. However, some modifications of the methods used here will be needed to accommodate the more complex nature of a full three-dimensional general circulation model.

[7] Ice/ocean coupled simulations are run for the above mentioned SHEBA case study. More specifically, the simulations are driven with forcing from SHEBA for 5 July–8 August 1998. The model used in this study is a single column ice/ocean mixed layer version of the Community Climate System Model 2 (CCSM2). It is described in section 2. The SHEBA observations during the case study are discussed in section 3. Results from the simulations are discussed in section 4. A discussion and the conclusions follow in section 5.

2. Model Description

[8] The model used in this study is a single column sea ice/ocean mixed layer version of the CCSM2. The model

represents a Lagrangian parcel moving with the SHEBA ice camp. Although the ice camp moved into different water mass structures, essentially representing an advective oceanic flux for the Lagrangian column, this is not accounted for in the model. This choice was made because good estimates of the advective fluxes are not available from SHEBA. This study attempts to isolate key processes and features that are needed to more accurately represent subgridscale lead processes. As such, the lack of advective fluxes in the model simulations and the discrepancies that this causes with the SHEBA observations are not critical to the conclusions from this study.

[9] A complete description of the full ice model is available from the National Center for Atmospheric Research at <http://www.cesm.ucar.edu/models/ice-csim4>. For this study a single-column system has been extracted from the full model. As such, the dynamic component of the original model is not used. Instead, strain rates are applied as external forcing in order to drive ridging and divergence in the Lagrangian column. Here a brief description of the relevant model physics is given. The sea ice model includes an ice thickness distribution based on the work of Thorndike *et al.* [1975], Rothrock [1975], and Bitz *et al.* [2001]. Five ice and a single open water category are included in the distribution. Ice-atmosphere and ice-ocean fluxes are computed for each category. Linear remapping [Lipscomb, 2001] is used to redistribute ice among thickness categories due to melt or growth. The model uses the thermodynamics of Bitz and Lipscomb [1999], which accounts for the effects of brine pockets within the sea ice. The lateral melt rate is parameterized following Maykut and Perovich [1987] and depends on the elevation of the water temperature above the freezing point. Lateral melting reduces the fractional area of sea ice following Rothrock and Thorndike [1984] and Steele [1992]. This parameterization accounts for the lateral surface area of ice floes through the use of an average floe diameter. In this study a constant average floe diameter of 300 m is used, which is probably typical for the central Arctic. The basal ice/ocean heat exchange is parameterized based on boundary layer theory following McPhee [1992]. It uses a constant transfer coefficient and is a function of the elevation of the water temperature above the freezing point and the skin friction velocity.

[10] The ocean boundary layer model used here is described fully by Large *et al.* [1994]. This model is currently incorporated into the CCSM2 ocean general circulation model. It resolves properties within the boundary layer and uses a nonlocal K profile parameterization (KPP) following Troen and Mahrt [1986] which was originally developed for the atmospheric boundary layer. This method assumes that the vertical turbulent fluxes depend on down-gradient diffusion. The parameterized diffusivity is consistent with similarity theory in the surface layer. The determination of the boundary layer depth utilizes a modified bulk Richardson number which depends on the surface forcing and the ocean buoyancy and velocity profiles.

[11] Three different configurations of the coupled ice/ocean system are used in this study (Figure 1). A brief description of these configurations is given in Table 1. These different methods of representing the ice/ocean system are relatively simple and are designed to provide guidance into how to improve lead processes within climate

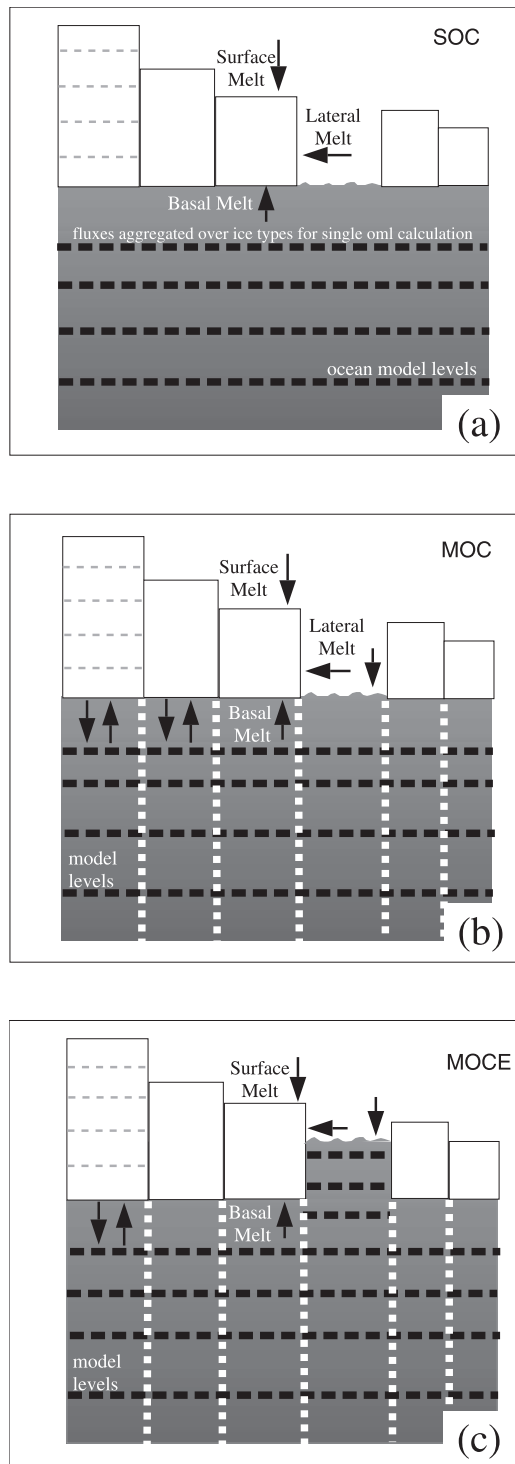


Figure 1. A schematic of the three different model configurations used in this study. In the SOC configuration a single ocean mixed layer calculation is performed. For the MOC and MOCE configurations, multiple ocean columns are represented and an ocean mixed layer calculation is performed for each ice type. The MOC and MOCE cases differ in that the MOCE case explicitly represents the lead surface which is embedded within the ice cover.

Table 1. Description of the Model Configurations Used in the Study

Name	Description
SOC	Single ocean column with one mixed layer calculation using fluxes aggregated over the ice thickness distribution
MOC	Multiple ocean columns simulated under each ice and open water type. Assumed that the lead and under-ice surface ocean are at the same depth.
MOCE	Same as MOC except the lead surface is embedded within the ice cover.

models. In the first of these, referred to as SOC, a single ocean column is present and one mixed layer calculation is performed. This uses the traditional climate modeling method of coupling in which fluxes are aggregated over the ice thickness and open water categories and a single value is provided to the ocean mixed layer for each flux component (e.g., heat, water, and momentum). In the second configuration, referred to as MOC, multiple ocean columns are present. Ocean mixed layer calculations are performed under each ice type and local ice/ocean fluxes are provided. It is assumed that the top grid point in the lead ocean column is at the same depth as the first under ice grid point. The under ice columns are laterally mixed every timestep, and the ice and lead columns are laterally mixed every N timesteps, where the typical timestep used is thirty minutes. In the standard simulations, N is equal to 12, resulting in mixing every 6 hours. The sensitivity to this value of N was tested and found to be considerable for this configuration. However, for the third model configuration, described below, the sensitivity was minimal. In the third model configuration, ocean mixed layer calculations are again performed under each ice type using local fluxes. However, in contrast to method two, the surface of the lead is embedded within the ice cover. Thus when lateral oceanic mixing is performed, the lead surface is isolated from the surrounding under-ice columns. This configuration is referred to as MOCE (Multiple Ocean Columns Embedded leads). In the standard MOCE runs, the uppermost three model levels (3 m) of the lead are “embedded” within the ice cover. This was chosen as a layer that would potentially be influenced by the ice cover. The model results are relatively insensitive to this parameter value as long as two or more model levels are in the protected portion of the lead. The mean ice thickness remains above 2 m and the fraction of ice thicker than 2.5 m ranges from 37% to 24% over the course of the integration. This suggests that “embedding” the uppermost three model levels of the lead within the ice cover is reasonable for this integration.

[12] The model is run with a 30 min timestep and 1 m resolution. The ocean model extends to 150 m depth, and the conditions are fixed at the bottom of the ocean column. The initial ocean conditions are obtained from the SHEBA under-ice CTD and lead profiles. Because the lead profiles only extend to 15 m depth, the conditions below this depth are set equal to those under the ice. There is no thickness distribution information available from SHEBA for the time period of this case study. Thus the sea ice initial conditions are obtained from a longer single column model integration which was run for the SHEBA year, forced with SHEBA observations, and initialized with SCICEX ice thickness

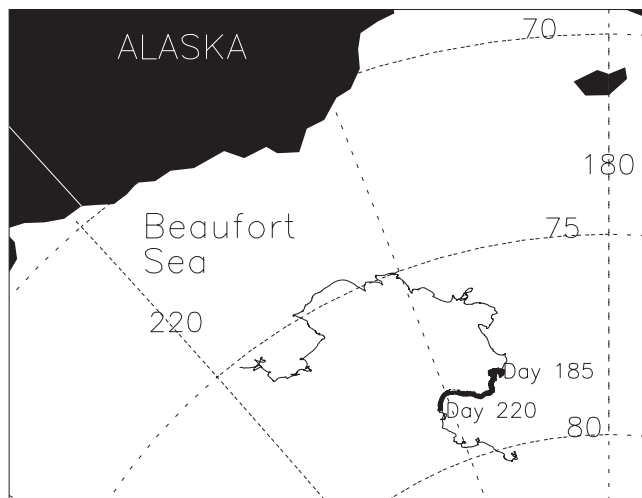


Figure 2. The position of the SHEBA camp with the case study period in bold and the beginning and end days of the case study noted.

observations. Some aspects of the simulations are sensitive to the initial ice thickness distribution conditions. In particular the amount of open water formed due to vertical melting shows a 1–2% increase in integrations with a 2% increase in the initial thin (<1.4 m) ice cover. However, the initial ice thickness distribution does not have a large influence on how the different model configurations compare or on the change in open water formation due to lateral melting. Thus the uncertainty in these conditions does not have an undue impact on the conclusions from this study.

3. SHEBA Observations

[13] The observations taken during the SHEBA field study are discussed by *Uttal et al.* [2002]. Simulations are performed for a case study using SHEBA forcing from 5 July–8 August 1998. This period was chosen because of the availability of lead observations and the interesting oceanic conditions that occurred. The forcing used in the model simulations consists of hourly wind speed, radiative fluxes, air temperature, precipitation, and sea ice strain rates. The forcing fields were taken from a variety of different measurement platforms and were compiled by *Curry et al.* [2001] for forcing a single column model such as the one used here. The atmospheric fields are discussed further by *Andreas et al.* [1999]. The turbulent ice/atmosphere fluxes are computed using standard bulk formulae (available at <http://www.cesm.ucar.edu/models/ice-csim4>). The strain rates which are used to drive the ice kinematics, including ice divergence and ridging, were obtained from the Radarsat Geophysical Processor Suite (RGPS) and are discussed further by *Stern and Moritz* [2002].

[14] At the beginning of the case study time period the ice camp was located in shallow water over the Chukchi cap (Figure 2). Over the course of the 5 week time period, the camp drifted over complex bathymetry and finally into deeper water (Figure 3). It is likely that changes in ocean conditions are associated with this changing bathymetry, and indeed climatological observations suggest that this is

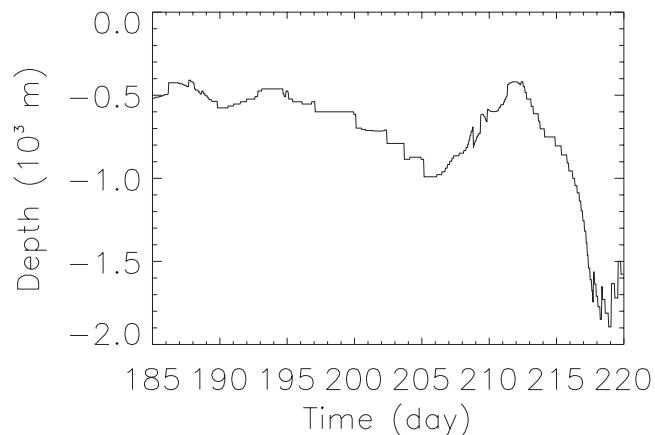


Figure 3. The bathymetry for the SHEBA camp over the case study period.

the case. In particular the Environmental Working Group Atlas [*Arctic Climatology Project*, 1998] indicates that a freshening occurs in the climatological conditions along the SHEBA drift track for this period (Figure 4). However, the advective fluxes associated with the camp drift are difficult to separate from the local ice/ocean exchange. As such, advective oceanic fluxes are not applied in the model simulations which will result in some discrepancy in the comparison of the model results and the observations.

[15] Measurements were taken in a small lead approximately 1 km WNW of the SHEBA ship adjacent to first year ice at the Sarah's Lake site [*Paulson and Pegau*, 2001; Pegau and Paulson, submitted manuscript, 2003]. These observations show a sharp decrease in salinity and increase in temperature in the upper 1 m of the lead from day 190–200 (Figure 5). Pegau and Paulson (submitted manuscript, 2003) discuss the evolution of these conditions within the lead and show that the low surface salinity is materialized as a freshwater layer which rapidly increased in thickness between day 191 and 198. The freshwater layer then stabilized at greater than 1 m depth. The lead surface stayed

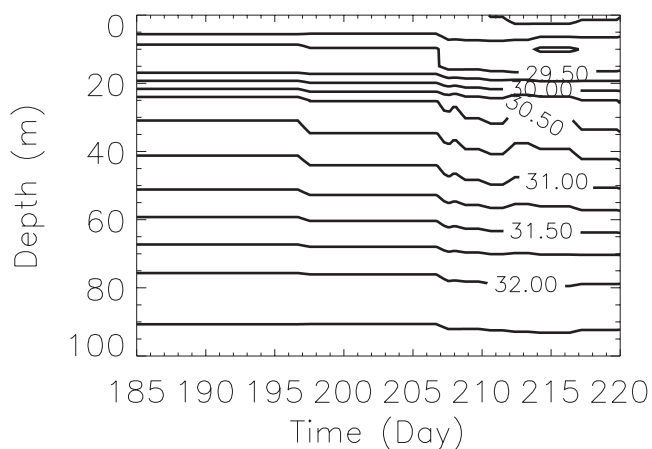


Figure 4. The salinity along the SHEBA drift track for the case study period from the Environmental Working Group Atlas.

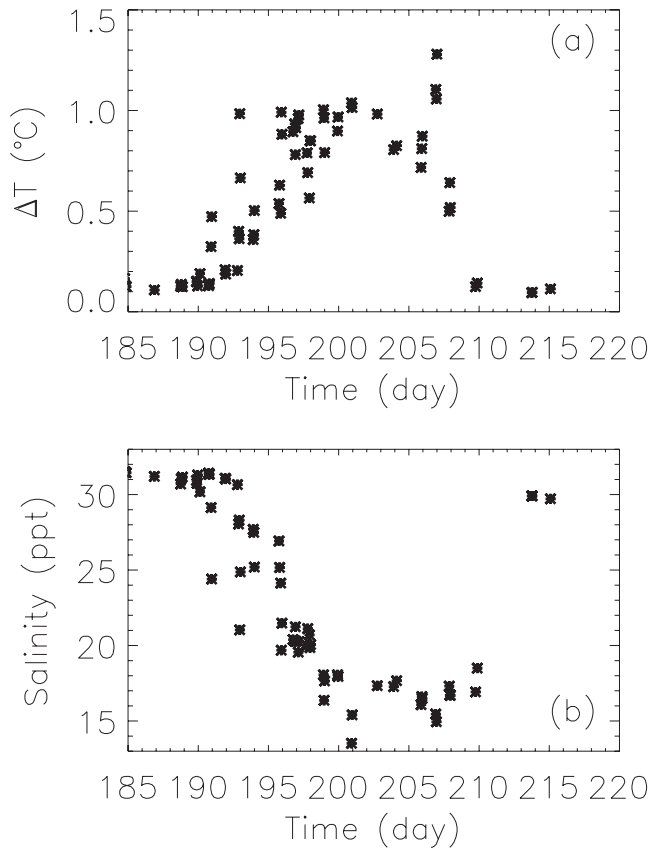


Figure 5. The observed (a) elevation of temperature above the freezing point (ΔT) and (b) salinity at the surface of the leads.

warm and fresh until approximately day 210 when it reverted to colder more saline conditions. Additional temperature and salinity measurements over this time period were made in the upper 2 m of a lead in the vicinity of undeformed multiyear ice at the Seattle site and for four helicopter lead surveys [Richter-Menge *et al.*, 2001]. These data all show similar conditions, suggesting that the lead conditions shown in Figure 5 are representative of the aggregate scale.

[16] These features of the lead surface appear to be strongly related to the wind forcing during this time period. Figure 6 shows the 10 m wind speed at the SHEBA camp [Andreas *et al.*, 1999]. A prolonged period of calm winds is present from day 191 to day 207 (Figure 6). This reduced the wind stirring in the lead and, in addition to the influx of surface meltwater and solar radiation, allowed for the rapid surface freshening and warming to occur. Around day 210, strong winds presumably caused the warm, fresh lead water to be mixed downward. As discussed by Perovich *et al.* [2003], lateral melting associated with leads at the SHEBA site was variable over the course of the melt season and was sizable for some time periods. For example, in early August, lateral melting accounted for approximately 29% of the change in ice mass, while basal melting contributed 49% and the remainder was due to surface melting.

[17] The under-ice temperature and salinity profiles [e.g., McPhee *et al.*, 1998] over the case study time period are shown in Figure 7. The upper water column gradually

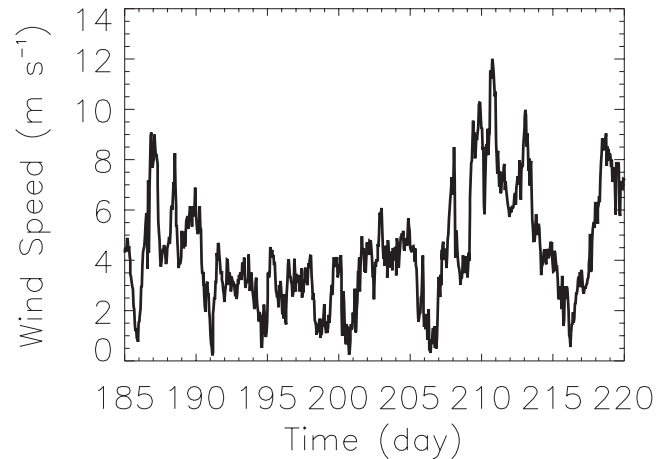


Figure 6. The observed wind speed at the SHEBA site.

warmed and freshened from day 185–207. Over the upper 80 m of the water column, this freshening is equivalent to the melting of approximately 0.6 m of sea ice, or an average melt rate of 2.5 cm/day. This is consistent with average melt rates for this time period as discussed by Perovich *et al.* [2003], indicating that local ice/ocean exchange was likely responsible for much of the upper water column changes over this time. However, from day 209–214, more dramatic

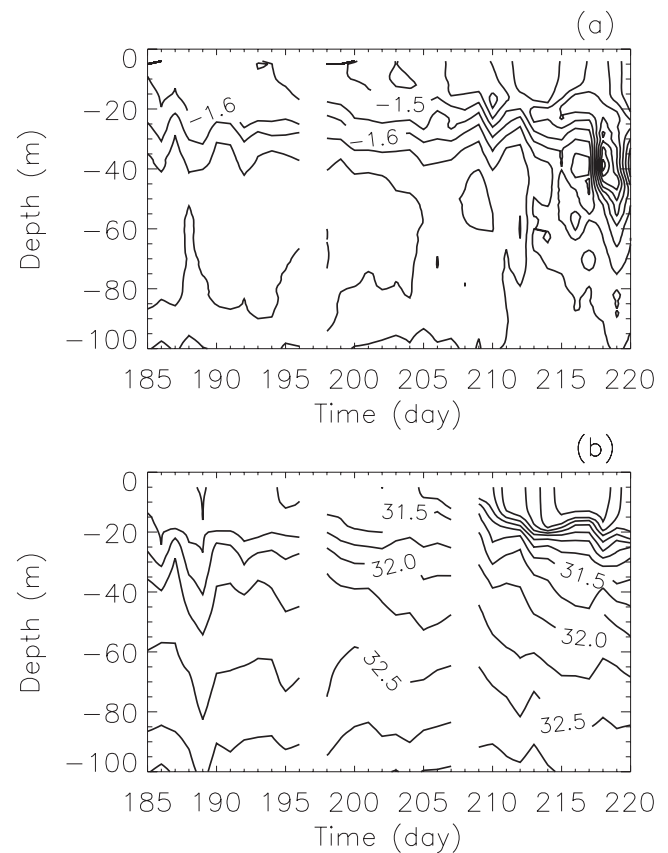


Figure 7. The observed under-ice (a) temperature and (b) salinity at the SHEBA site. The contour interval is 0.05°C for temperature and 0.25 ppt for salinity.

changes were observed. In particular the water column significantly warmed and freshened in the upper 80 m. It is likely that some of this was related to the mixing down of the warm, fresh lead water. However, the change in salinity over this short time period amounts to an average ice melt rate of approximately 27 cm/day. This is about an order of magnitude larger than the maximum melt rates at any time during the melt season [Perovich *et al.*, 2003] and, as discussed above, advective fluxes or other processes such as the trapping and subsequent flushing of meltwater in under-ice melt ponds [e.g., Eiken, 1994] are necessary to explain the observed changes.

4. Model Results

[18] Ocean general circulation models typically do not differentiate between ice-covered and ice-free portions of a grid cell. Instead, they use a flux that is aggregated over different surface types. Hence these models are not able to simulate the types of lead conditions discussed above. This can have implications for the ice mass balance and climate feedbacks in these models.

[19] In an effort to isolate the important characteristics that are associated with the subgridscale mixing of summertime leads, three different model configurations are used to simulate the ice/ocean conditions. These configurations are discussed in section 2 (Table 1, Figure 1). As mentioned above, owing to the difficulties in diagnosing lateral ocean exchange from the SHEBA observations, these simulations do not apply advective fluxes. Instead, all simulated changes in ocean conditions result from local ice/ocean/atmosphere exchange. This will result in some discrepancies between the simulated and observed oceanic conditions.

[20] Figure 8 shows the surface (1 m) lead conditions obtained using the three different model configurations and the observations. Simulations which use a single ocean-mixed layer (SOC) calculation or multiple ocean-mixed layer calculations with no embedded leads (MOC) obtain similar results, reaching minimum salinities of 28.9 and 28.5 ppt and maximum elevations of temperature above the salinity determined freezing point (ΔT) of 0.20 and 0.35°C, respectively. However, when the ice is submerged below the waterline and the surface of the lead is realistically embedded within the ice cover using configuration MOCE, considerably different conditions result. In particular, the lead surface is allowed to rapidly warm and freshen as seen in the observations. When stabilizing conditions occur, as they did during this time period, the simulated oceanic boundary layer in the lead is very shallow (less than a meter in MOCE). Because the lead is embedded within the ice cover, there is no direct, lateral mixing between the lead surface and the under-ice ocean system. Thus under stable conditions, the lead surface remains isolated and is able to accumulate meltwater runoff. This results in a decrease in salinity to 20.2 ppt and an increase in ΔT to greater than 1.4°C. As the wind speed increases, mechanical forcing causes an increase in the boundary layer depth, until the surface lead conditions are well mixed to a sufficient depth to be in “communication” with the under-ice system. The lead surface consequently cools to 0.13°C above freezing and becomes more saline, reaching a value of 31.7 ppt on day 220.

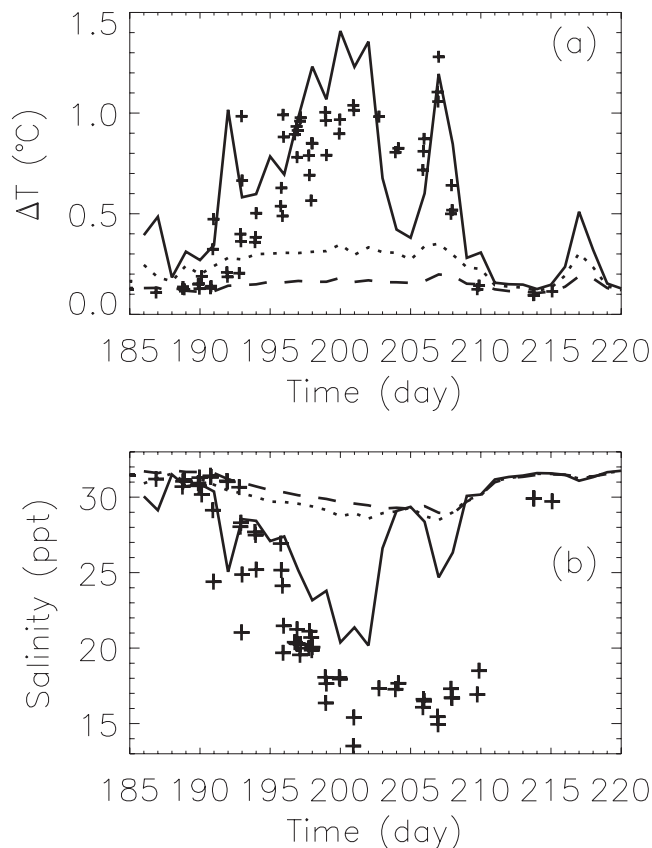


Figure 8. The simulated (a) elevation of temperature above the freezing point (ΔT) and (b) salinity at the surface of the leads for the three model configurations (dashed line is SOC, dotted line is MOC, and solid line is MOCE). The observations are shown as plus signs.

[21] The MOCE configuration obtains a very reasonable simulation of the lead conditions given the level of simplicity of the model system. It obtains many of the features of the observed leads both in the timing of events and in the magnitude of certain properties. For example, the heat content in the upper meter of the lead for day 190–210 differs by only 15% between the simulated and observed values. This heat content is what ultimately affects the simulated lateral melt rates, indicating that reasonable thermodynamically driven open water formation is possible in this simulation. This is discussed further below.

[22] The MOCE model solutions do show some notable differences from the observations. In particular the observed lead conditions are considerably fresher than those simulated by the model for days 197–210 and the model obtains a considerably larger decrease in ΔT and increase in salinity around day 203–204 than is present in the observations. There are a number of model uncertainties that could contribute to this bias, including errors in the simulated melt rates, meltwater runoff, and general freshwater and heat budgets of the leads. Additionally, the model resolution may be inadequate to accurately simulate the structure of the surface freshwater layer in the lead which, as indicated by Pegau and Paulson (submitted manuscript, 2003), can be quite thin. Finally, there are a number of processes/properties that the model greatly simplifies or does not capture at

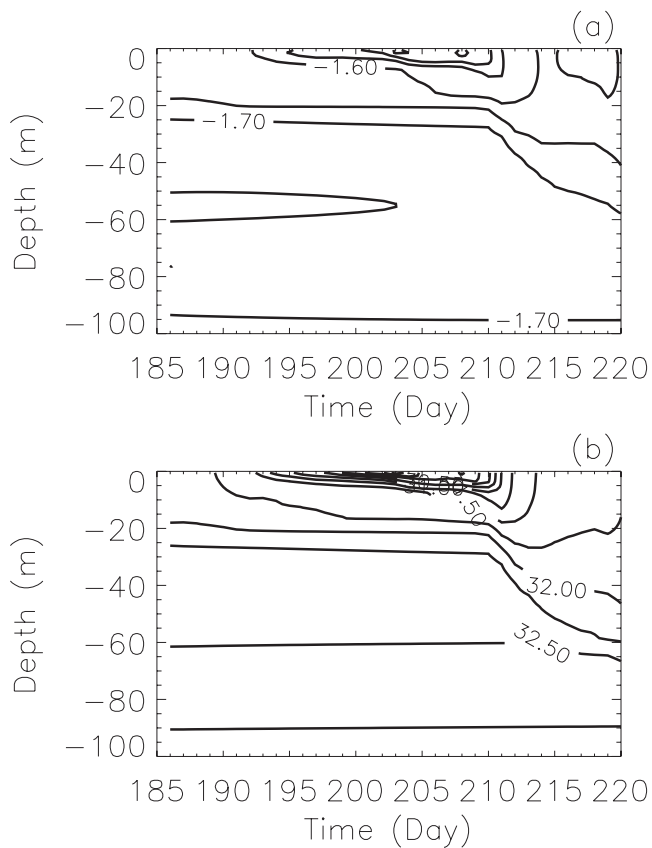


Figure 9. The simulated under-ice (a) temperature and (b) salinity profiles for the MOCE configuration. The contour interval is 0.05°C for temperature and 0.25 ppt for salinity.

all. For example, leads and the surrounding ice cover have a very complicated morphology, including ice overhangs above the waterline, ice shelves below the waterline, and a complex lead perimeter structure. These details, which are not accounted for in the model, influence the exchange of heat and freshwater between the lead and ice cover. In light of these model simplifications the agreement with the observations is very good and gives great promise that the MOCE configuration can be adapted for and used in climate models to considerably improve the representation of summertime lead processes. Adapting this configuration to a climate model will require that it is compatible with regions (e.g., grid cells) that are completely ice free and that it accounts for the three-dimensional nature of an ocean general circulation model. This is discussed further in section 5.

[23] Associated with the mixing down of the lead water, the under-ice oceanic conditions warm and freshen at depth around day 210 (Figure 9). This occurs in all of the simulations, although the source of this water is somewhat different. All of the simulations obtain a gradual warming and freshening of the under-ice surface conditions until day 210. In the SOC and MOC simulations, these changes in under-ice surface conditions are larger than in the MOCE case with embedded leads. In all of the simulations the under-ice conditions are affected by basal melting and solar radiation which penetrates through the sea ice. However, in the MOCE run, during the period of calm winds, the lateral

and surface meltwater and absorbed solar flux are largely confined to the leads. In contrast, in the SOC and MOC model configurations, these fluxes directly affect the under-ice conditions. It is difficult to assess which of these under-ice simulations is “best” compared with the SHEBA observations. They all obtain the general characteristics of the SHEBA observations. However, some considerable differences occur. In particular, the large surface freshening and subsurface warming that occurred around day 210 in the observations are not present in the model simulations which instead obtain increasing surface salinity after day 210. Additionally, the observations show a very warm small-scale feature around day 218 centered at approximately 40 m depth which is not simulated. As discussed in section 3, these features in the observations are likely affected by oceanic advection as the SHEBA camp moved over the complex bathymetry of the Chukchi cap. These advective effects are neglected in the model simulations. Additionally, processes associated with, for example, under-ice melt ponds and variable surface meltwater drainage are not included in the model simulations and may have affected the observed conditions.

[24] The large differences in the surface lead conditions between the embedded lead case and other configurations cause differences in the lateral melt rates and open water formation to occur (Figure 10). With the SOC and MOC model configurations, very little open water formation is produced by lateral melting and the average lateral melt rate from day 185–199 for an individual lead is only 1 – 2 cm/day. However, with the very warm lead conditions simulated by MOCE, the lateral melt rates are sizable, averaging 10 cm/day from day 185–199. In light of expected spatial inhomogeneity at the SHEBA site this simulated value agrees very well with the observed 16 cm/day obtained from a mass balance study at a single lead site [Perovich *et al.*, 1999].

[25] The large lateral melt rates simulated by the MOCE case affect the open water fraction within the model domain, resulting in a 4% increase in the open water area. This

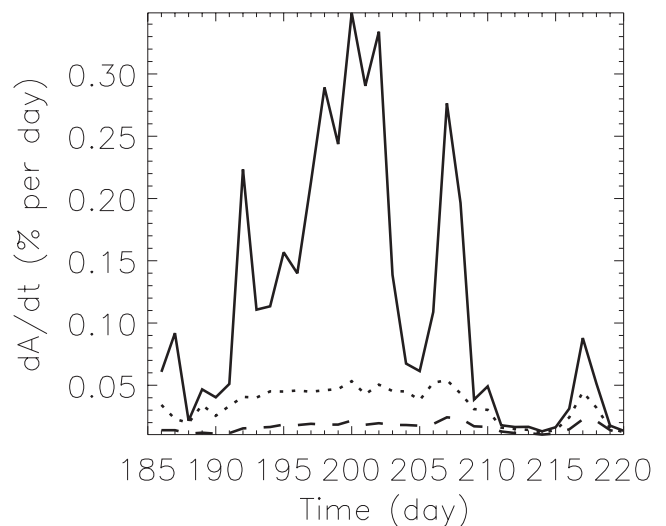


Figure 10. The simulated rate of change of open water formation due to lateral melting (dashed line is SOC, dotted line is MOC, and solid line is MOCE).

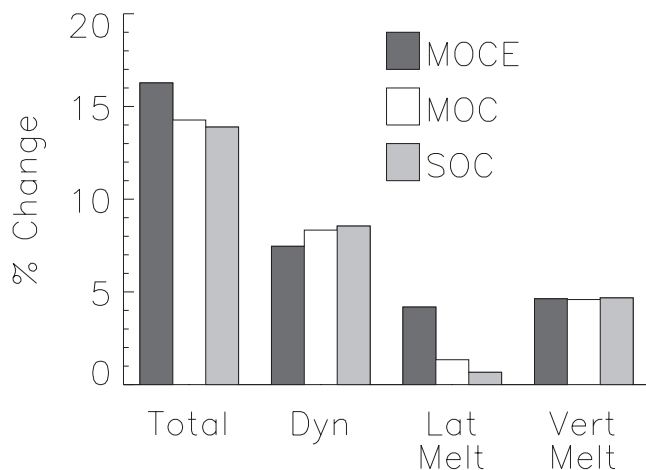


Figure 11. The open water budgets for the three different model configurations. Included are the total change in open water fraction (Total) and the change in open water fraction due to dynamical processes (Dyn), lateral melting (Lat Melt), and vertical melting (Vert Melt) over the integration period.

accounts for approximately 26% of the total change in open water over the simulation period (Figure 11). This is in contrast to the MOC and SOC simulations in which lateral melting only accounts for 9% and 5% of the total open water change, respectively. The remainder of the change in open water is caused by dynamical processes (including ice divergence, convergence, and shear), which accounts for 46% of the total, and vertical melting, which accounts for 28% of the total in the MOCE integration. The open water formation due to vertical melting is similar regardless of the model configuration, whereas dynamical processes have a reduced effect on the open water budgets in the MOCE integration compared with the other simulations. Nonetheless, considerably more open water is obtained using the MOCE configuration, with the open water fraction increasing from 6.7% to 19.2% from day 190 to day 220 for a total increase of 12.5%. This compares very well to observational estimates of a 12.9% change in open water fraction over the same time period [Tschudi *et al.*, 2001; Perovich *et al.*, 2002].

[26] The increased open water formation that results from lateral melting in the MOCE integration has a strong albedo feedback associated with it. In particular, it causes a 15–20% increase in absorbed solar radiation in the ocean over the 41 day simulation period as compared with the other configurations. This suggests that the ability to simulate the type of warm and fresh conditions observed in the leads during SHEBA may have implications for the accurate modeling of climate change and variability through their influence on the albedo feedback.

5. Discussion and Conclusions

[27] Ocean and sea ice general circulation models (GCMs) have made significant advancements in recent years. However, there are many subgridscale processes associated with the ice/ocean system that are poorly represented. In particular, although many climate models now allow for leads or

cracks within the ice cover, they still assume that the open water and under-ice ocean systems are well mixed and apply only a single aggregated ice/ocean/atmosphere flux. Previous studies and recent observations from the SHEBA field study suggest that these assumptions are invalid for both the ocean and atmosphere systems. This can influence the simulation of the albedo and cloud feedback mechanisms within climate models and modify simulations of climate variability and change.

[28] This study investigates methods to improve the representation of subgridscale effects of summertime leads on the ocean system. This was motivated in part by the SHEBA observations of Pegau and Paulson (submitted manuscript, 2003) which show remarkably fresh and warm conditions occurring at the surface of summertime leads. Under calm wind conditions, the lead and under-ice ocean columns were clearly not well mixed during SHEBA, indicating that GCM representations of these systems are flawed. The observed stable lead conditions during SHEBA allowed for considerable heat storage in the leads. This influenced lateral melt rates, open water formation [Perovich *et al.*, 2003], and ultimately the surface albedo.

[29] Simulations of these conditions were performed using a single-column ice/ocean mixed layer model driven by SHEBA observations. The purpose of these simulations was to isolate important properties of the leads that were needed to improve the representation of the subgridscale lead effects for climate modeling. As such, model components from the Community Climate System Model were extracted and run in a single-column framework. Three different model configurations were used. These include (1) a traditional method in which a single mixed layer calculation was driven by an aggregate flux, (2) a method in which mixed layer calculations were performed under each ice type, and (3) a method that was identical to the second except that the lead surface was embedded within the ice cover.

[30] The model results show that in order to obtain the types of conditions seen in the observations, the ocean system must explicitly differentiate between ice-covered and open water regions. Additionally, it is necessary for the surface of the lead to be realistically embedded within the ice cover. Under stable conditions this allows the lead surface to remain isolated from the rest of the ocean and can result in very fresh and warm conditions, with surface salinities approaching 20 ppt and surface temperatures elevated over 1.4°C above freezing. The model results clearly show that this modifies the lateral melt rates and open water formation which consequently decreases the surface albedo, allowing 15–20% more absorbed solar radiation compared with the cases without embedded leads. This indicates that a better representation of lead processes in climate models can modify the simulated albedo feedback which will influence the simulation of climate change and variability. It should be noted that dynamic effects also modify the summertime open water formation. These effects have been included in this study through the application of strain rate forcing which drives open water formation and ridging. Additionally, there are feedbacks between dynamic and thermodynamic open water formation that can modify the simulated open water formation. These feedbacks have not been considered here.

[31] The results of this study suggest that the stabilizing conditions present in summertime leads can be important for climate in that they can modify important feedback mechanisms. Because of these effects, it is important to assess the influence of these processes in climate models. The method used here to obtain improvements in the subgridscale mixing associated with summertime lead processes is promising for climate modeling in that it is relatively simple and does not represent an undue computational burden. The fact that the models used in this study are components of the Community Climate System Model (CCSM) should further simplify the extension of the methods described here to GCMs.

[32] Currently, the CCSM uses a traditional method for coupling the ice and ocean systems (as in configuration SOC). In future work this will be modified to allow for an open water and under-ice mixed layer calculation with an embedded lead surface. This requires a number of modifications to the CCSM ocean model component which must be general enough to work in ice-free and marginal ice zone regions. The results of this study suggest that two ocean mixed layer calculations (for leads and under-ice columns) are needed to represent the stable conditions that can exist at lead surfaces and how this interacts with the deeper ocean. However, it appears that the under-ice and lead columns can remain well mixed below the embedded lead region, requiring the storage of only a single ocean column plus information on 2–3 embedded lead points. The properties of the deeper column will need to be advected with the ocean currents, whereas properties of the embedded lead surface will not be transported. In open ocean grid cells, a single ocean mixed layer calculation is required. It is expected that this will use the same vertical resolution as is present in an under-ice column (e.g., excluding the embedded lead portion). This should allow for relatively straightforward transport between ice-covered and ice-free regions. When an ice-covered grid cell becomes open ocean, it will be necessary to mix the properties of the “embedded” lead water with the upper layer of the ocean column, representing a heat and water flux to the upper ocean. This will ensure conservation of these properties. It is anticipated that the actual method used to incorporate the MOCE configuration into a GCM will be revised based on experiments and sensitivity tests within the GCM context.

[33] **Acknowledgments.** The author would like to thank Bill Large, Peter Gent, and two anonymous reviewers for providing valuable comments on this manuscript and Scott Pegau for some useful email discussions. Thanks is also given to Cecilia Bitz who provided the single column version of the sea ice model. Special gratitude is extended to the participants in the SHEBA field program who have provided the research community with an invaluable data set and research tool. The research was supported as part of the SHEBA phase III project by a National Science Foundation grant and by the International Arctic Research Center. NCAR is supported by the National Science Foundation.

References

- Andreas, E. G., C. W. Fairall, P. S. Guest, and P. O. G. Persson, An overview of the SHEBA atmospheric surface flux program, paper presented at Fifth AMS Conf. on Polar Meteorol. and Oceanogr., Dallas, Tex., 10–15 January 1999.
- Arctic Climatology Project, *Environmental Working Group Joint U.S.-Russian Atlas of the Arctic Ocean—Summer Period* [CD-ROM], edited by L. Timokhov and F. Tanis, Environ. Res. Inst. of Michigan, Ann Arbor, Mich., 1998.
- Badgley, F., Heat budget at the surface of the Arctic Ocean, *Proceedings of the Symposium on the Arctic Heat Budget and Atmospheric Circulation*, edited by J. O. Fletcher, pp. 267–277, Rand Corp., Santa Monica, Calif., 1966.
- Bitz, C. M., and W. H. Lipscomb, An energy-conserving thermodynamic model of sea ice, *J. Geophys. Res.*, *104*, 15,669–15,677, 1999.
- Bitz, C. M., M. M. Holland, M. Eby, and A. J. Weaver, Simulating the ice-thickness distribution in a coupled climate model, *J. Geophys. Res.*, *106*, 2441–2463, 2001.
- Curry, J. A., J. L. Schramm, D. Perovich, and J. O. Pinto, Application of SHEBA/FIRE data to evaluation of sea ice surface albedo parameterizations, *J. Geophys. Res.*, *106*, 15,345–15,355, 2001.
- Eiken, H., Structure of under-ice melt ponds in the central Arctic and their effect on the sea ice cover, *Limnol. Oceanogr.*, *39*, 682–694, 1994.
- IPCC, *Climate Change 2001: The Scientific Basis, Contribution of Working Group I to the Third Assessment Report of the Intergovernmental Panel on Climate Change*, edited by J. T. Houghton et al., 881 pp., Cambridge Univ. Press, New York, 2001.
- Kantha, L. H., A numerical model of Arctic leads, *J. Geophys. Res.*, *100*, 4653–4672, 1995.
- Large, W. G., J. C. McWilliams, and S. C. Doney, Oceanic vertical mixing: A review and a model with a vertical K-profile boundary layer parameterization, *Rev. Geophys.*, *32*, 363–403, 1994.
- Lipscomb, W. H., Remapping the thickness distribution in sea ice models, *J. Geophys. Res.*, *106*, 13,989–14,000, 2001.
- Maykut, G. A., Large-scale heat exchange and ice production in the central Arctic, *J. Geophys. Res.*, *87*, 7971–7984, 1982.
- Maykut, G. A., and M. G. McPhee, Solar heating of the Arctic mixed layer, *J. Geophys. Res.*, *100*, 24,691–24,703, 1995.
- Maykut, G. A., and D. K. Perovich, The role of shortwave radiation in the summer decay of a sea ice cover, *J. Geophys. Res.*, *92*, 7032–7044, 1987.
- McPhee, M. G., Turbulent heat flux in the upper ocean under sea ice, *J. Geophys. Res.*, *97*, 5365–5379, 1992.
- McPhee, M. G., and T. P. Stanton, Turbulence in the statically unstable ocean boundary layer under Arctic leads, *J. Geophys. Res.*, *101*, 6409–6428, 1996.
- McPhee, M. G., T. P. Stanton, J. H. Morison, and D. G. Martinson, Freshening of the upper ocean in the Arctic: Is perennial sea ice disappearing?, *Geophys. Res. Lett.*, *25*, 1729–1732, 1998.
- Morison, J. H., M. G. McPhee, T. B. Curtin, and C. A. Paulson, The oceanography of winter leads, *J. Geophys. Res.*, *97*, 11,199–11,218, 1992.
- Paulson, C. A., and W. S. Pegau, The summertime thermohaline evolution of an Arctic lead: Heat budget of the surface layer, in *Preprints, Sixth Conference on Polar Meteorology and Oceanography*, pp. 271–274, Am. Meteorol. Soc., San Diego, Calif., 2001.
- Perovich, D. K., T. C. Grenfell, B. Light, J. A. Richter-Menge, M. Sturm, W. B. Tucker III, H. Eiken, G. A. Maykut, and B. Elder, *SHEBA: Snow and Ice Studies* [CD-ROM], Cold Regions Res. and Eng. Lab., Hanover, N. H., 1999.
- Perovich, D. K., W. B. Tucker III, and K. A. Ligett, Aerial observations of the evolution of ice surface conditions during summer, *J. Geophys. Res.*, *107*(C10), 8048, doi:10.1029/2000JC000449, 2002.
- Perovich, D. K., T. C. Grenfell, J. A. Richter-Menge, B. Light, W. B. Tucker III, and H. Eiken, Thin and thinner: Ice mass balance measurements during SHEBA, *J. Geophys. Res.*, *108*, doi:10.1029/2001JC001079, in press, 2003.
- Pinto, J. O., J. A. Curry, and K. L. McInnes, Atmospheric convective plumes emanating from leads, I: Thermodynamic structure, *J. Geophys. Res.*, *100*, 4621–4631, 1995.
- Pinto, J. O., A. Alam, J. A. Maslanik, and J. A. Curry, Characteristics and atmospheric footprint of springtime leads at SHEBA, *J. Geophys. Res.*, *108*, doi:10.1029/2000JC000473, in press, 2003.
- Rothrock, D. A., The energetics of the plastic deformation of pack ice by ridging, *J. Geophys. Res.*, *80*, 4514–4519, 1975.
- Rothrock, D. A., and A. S. Thorndike, Measuring the sea ice floe size distribution, *J. Geophys. Res.*, *89*, 6477–6486, 1984.
- Serreze, M. C., J. D. Kahl, E. L. Andreas, J. A. Maslanik, M. C. Rehder, and R. C. Schnell, Theoretical heights of buoyant convection above open leads in the winter arctic pack ice cover, *J. Geophys. Res.*, *97*, 9411–9422, 1992.
- Skillingstad, E. D., and D. W. Denbo, Large eddy simulation of turbulence under sea ice and leads, *J. Geophys. Res.*, *106*, 2477–2498, 2001.
- Smith, D. C., IV, and J. H. Morison, Nonhydrostatic haline convection under leads in sea ice, *J. Geophys. Res.*, *103*, 3233–3247, 1998.
- Steele, M., Sea ice melting and floe geometry in a simple ice-ocean model, *J. Geophys. Res.*, *97*, 17,729–17,738, 1992.
- Stern, H. L., and R. E. Moritz, Sea ice kinematics and surface properties from RADARSAT SAR during the SHEBA drift, *J. Geophys. Res.*, *107*(C10), XXXX, doi:10.1029/2000JC000472, 2002.

- Thorndike, A. S., D. S. Rothrock, G. A. Maykut, and R. Colony, The thickness distribution of sea ice, *J. Geophys. Res.*, *80*, 4501–4513, 1975.
- Troen, I. B., and L. Mahrt, A simple model of the atmospheric boundary layer: Sensitivity to surface evaporation, *Boundary Layer Meteorol.*, *37*, 129–148, 1986.
- Tschudi, M. A., J. A. Curry, and J. A. Maslanik, Airborne observations of summertime surface features and their effect on surface albedo during FIRE/SHEBA, *J. Geophys. Res.*, *106*, 15,335–15,344, 2001.
- Uttal, T., et al., Surface heat budget of the Arctic Ocean, *Bull. Amer. Meteor. Soc.*, *83*, 255–275, 2002.
-
- M. M. Holland, National Center for Atmospheric Research, Climate and Global Dynamics Division, P.O. Box 3000, Boulder, CO 80307-3000, USA. (mholland@ucar.edu)